International Journal of Biological Macromolecules 276 (2024) 133850

Contents lists available at ScienceDirect

International Journal of Biological Macromolecules

journal homepage: www.elsevier.com/locate/ijbiomac

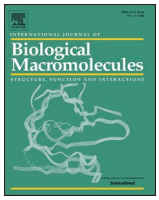

Mathematical modelling of genipin-bovine serum albumin interaction using fluorescence intensity measurements

Djurdja Vukajlovic [a], Rory Timmons [a], Stevan Macesic [b], John Sanderson [a], Fengwei Xie [a,c], Tarek M. Abdelghany [d,e,f], Emma Smith [g], Wing Man Lau [g], Keng Wooi Ng [g], Katarina Novakovic [a,*]

[a] School of Engineering, Newcastle University, Newcastle upon Tyne NE1 7RU, United Kingdom
[b] University of Belgrade, Faculty of Physical Chemistry, Studentski trg 12-16, Belgrade, Serbia
[c] Department of Chemical Engineering, University of Bath, Bath BA2 7AY, United Kingdom
[d] Department of Pharmacology and Toxicology, Faculty of Pharmacy, Cairo University, Kasr El-Aini St., Cairo 11562, Egypt
[e] Institute of Education in Healthcare and Medical Sciences, School of Medicine, Medical Sciences and Nutrition, University of Aberdeen, Foresthill, Aberdeen AB25 2ZD, United Kingdom
[f] School of Biomedical, Nutritional and Sport Sciences, Faculty of Medical Sciences, Newcastle University, Newcastle upon Tyne NE2 4HH, United Kingdom
[g] School of Pharmacy, Faculty of Medical Sciences, Newcastle University, Newcastle upon Tyne NE1 7RU, United Kingdom

ARTICLE INFO

Keywords:
Genipin
Bovine serum albumin
Kinetic fitting
Reaction network
Modelling
Fluorescence intensity

ABSTRACT

The interaction between genipin and a model protein bovine serum albumin (BSA), with and without the addition of acetic acid, has been studied experimentally and by modelling. The number of amino groups available to react was determined to be 5.6 % of the total number of amino acid building blocks on BSA. Fluorescence intensity was used to record the progress of the reaction over the 24 h, while the modelling study focused on capturing the kinetic profiles of the reaction. The experiments revealed a slow start to the BSA and genipin interaction, that subsequently accelerated in an S-shaped curve which the modelling study linked with the existence of the feedback cycle for both reactive amino groups and genipin. At BSA concentrations ≥30 mg/mL the reaction was accelerated in the presence of acid, while below 30 mg/mL the acidified conditions delayed the onset of the reaction. Contrary to the reaction mechanisms previously proposed, a degree of breakdown of the fluorescent links in the products formed was denoted both experimentally and in a modelling study. This indicated the reversibility of the processes forming fluorescent product/s and suggested feasibility of the successful release of the protein following prospective encapsulation within the genipin-crosslinked hydrogel structure.

1. Introduction

Recent advancements in biotechnology have led to a wide range of peptide and protein drugs for the prevention and treatment of various diseases. Examples include vaccines against infections, hormones (e.g., insulin for diabetes mellitus), as well as antibodies (e.g., nivolumab, rituximab) and cytokines (e.g., epoetin, interferons) against cancers and autoimmune disorders, among others. The most effective administration route for these advanced therapeutics is through parenteral injection due to their poor oral bioavailability caused by pre-systemic enzymatic degradation and low intestinal permeability [1,2]. However, the prolonged and frequent injections coupled with the prohibitive cost of medication and associated professional care, can reduce medication adherence due to factors such as patient discomfort, aversion to injections, concerns about needle size, and local irritation. Therefore, it is vital to develop alternative drug delivery technologies for peptide and protein drugs with a focus on patient acceptability and usability. Market trends indicate that the global market for oral peptide and protein drugs will grow from US$643 million in 2016 to US$8.23 billion in 2028. The total biologics market (valued at US$255.19 billion in 2019) is expected to increase with a compound annual growth rate of 7.6 % between 2019 and 2027 [3]. In response to the identified need, scientific groups have endeavoured to develop alternative formulations and routes for the delivery of protein and peptide drugs. This includes advanced oral, nasal, ophthalmic, buccal, and transdermal formulations as well as injectable and implantable formulations for prolonged drug dosing

* Corresponding author.
E-mail address: katarina.novakovic@newcastle.ac.uk (K. Novakovic).

https://doi.org/10.1016/j.ijbiomac.2024.133850
Received 30 August 2023; Received in revised form 10 July 2024; Accepted 11 July 2024
Available online 14 July 2024

[4,5].

The impetus behind the research here stems from growing interest in advancing hydrogel-based materials as scaffolds for protein and peptide drug delivery. Hydrogel scaffolds containing the drug of interest can be designed to protect it from the host environment and once in the desired location release it in a controlled manner [6]. To obtain stable hydrogel structures that can contain and subsequently release the drug, these constructs are frequently fabricated using cross-linking agents that enable the gel formation [7]. Chitosan-based hydrogels have garnered extensive research attention due to the promising properties of chitosan and its widespread availability and accessibility [8–10]. In the case of chitosan, cross-linking agents typically react with the amino groups present on chitosan (formed following chitin deacetylation) linking neighbouring chitosan chains and forming hydrophilic, porous three-dimensional structures [11]. Importantly, peptide and protein drugs can also engage their free amino groups in this reaction. While chemical binding of the drug to a hydrogel scaffold can have advantages such as extended drug containment and subsequent release upon scaffold degradation. It is important to understand this process and its kinetics to use it efficiently.

This study assesses the reaction of proteins with genipin, a cross-linking agent, by using bovine serum albumin (BSA) as a model protein. BSA often represents serum albumin proteins especially human serum albumin [12]. Genipin ($C_{11}H_{14}O_5$, 226.23 g/mol) is a white crystalline powder extracted from the *Gardenia jasminoides* plant, its solubility in distilled water is ~1 % *w/v* at 25 °C and 2 % w/v at 37 °C [13]. Naturally biocompatible, genipin has been a staple in Chinese medicine for centuries and is renowned for its various health benefits such as anti-inflammatory and diuretic effects [14]. In recent years, genipin has been increasingly used as a cross-linking agent to form chitosan-based hydrogels [15], where its low cytotoxicity compared to alternative cross-linking agents such as glutaraldehyde stands out [14,16]. On the other hand, BSA is a protein that makes up approximately 10 % of the total whey protein content in milk and is predominantly found in the bovine circulatory system. BSA comprises 583 amino acids residues with a molecular weight of 66.4 kDa [17] (Fig. S1, Supplementary Material). It is a widely accepted model protein due to its abundance, low cost, structural stability, similarity to other proteins and relevance to biological systems [18]. BSA molecules contain lysine and arginine residues with reactive primary amine groups. This makes it an ideal model protein to study for cross-linking with genipin [19].

2. Previous studies of genipin and bovine serum albumin reactions

Several studies have investigated genipin and BSA reactions aimed to form hydrogels and/or encapsulate and deliver proteins [14,16], [19–21]. Butler et al. studied the mechanism of the cross-linking reaction between biopolymers containing primary amine groups and genipin using FTIR, UV–Vis, ^{13}C NMR, protein-transfer reaction mass spectrometry, photon correlation spectroscopy and dynamic oscillatory rheometry [14]. They concluded that two reactions take place at different rates. The faster reaction is a nucleophilic attack on genipin by a primary amine group leading to the formation of a heterocyclic compound of genipin linked to the glucosamine residue in chitosan and the basic residues in BSA and gelatin (Reaction Scheme 2, Fig. 1). The second slower reaction was the nucleophilic substitution of the ester group possessed by genipin to form a secondary amide link with chitosan, BSA, or gelatin (Reaction Scheme 1, Fig. 1). Furthermore, after denoting a slower cross-linking reaction in the presence of deuterium oxide (in place of water), they concluded that acid catalysis was necessary for either or both reactions to proceed.

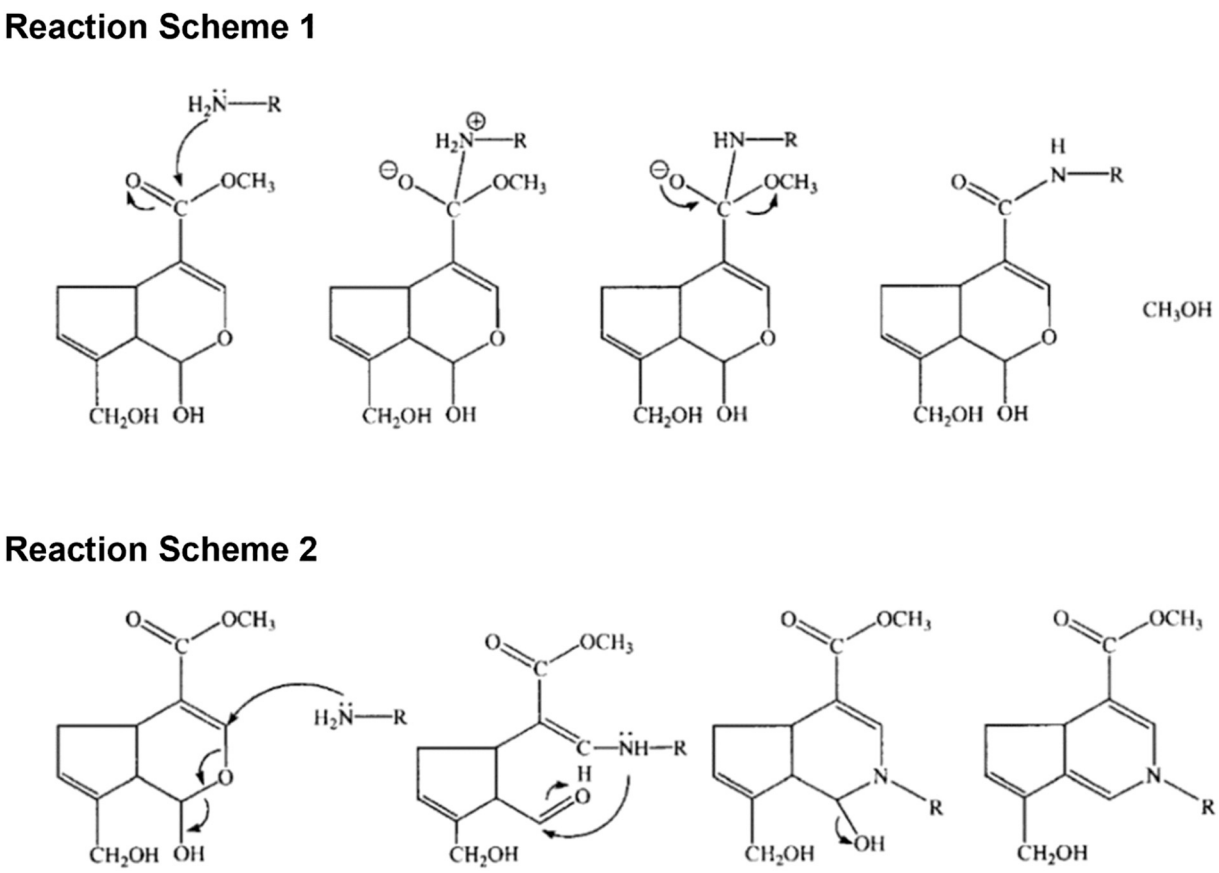

Fig. 1. Proposed mechanism of cross-linking reaction involving genipin and primary amine groups. Adapted from Butler et al. [14] with permission from John Wiley and Sons.

The interaction of primary amine with genipin is further studied by Chen et al. in a more complex system of pH-responsive hydrogels consisting of *N*,*O*-carboxymethyl chitosan (NOCC) and alginate cross-linked by genipin for controlled protein drug delivery. Where BSA as a model protein was added to the system during the hydrogel formation [16]. In this set-up, the primary amine groups on chitosan and BSA can both react with genipin during the gel formation which would be expected to impair the release of BSA. On the contrary, the amount of BSA released over 5 h was found to be a function of pH in the environment ranging from 20 % at pH 1.2 to 80 % at pH 7.4. Leading to a conclusion that the genipin-cross-linked NOCC/alginate hydrogel could be a suitable polymeric carrier for site-specific protein drug delivery in the intestine. Chen et al. also recognised the potential of genipin to cross-link a small amount of BSA. Their primary suggested the cross-linking route involves the reaction between NOCC and genipin as shown in Fig. 2. This is based on a previously proposed mechanism by Touyama et al. [22], where the initial nucleophilic attack at C3 is proposed in Reaction Scheme 2, Fig. 1 [14]. Following this, dimerisation is assumed to occur in the second step potentially via radical polymerisation.

Recently, Wang et al. reported a biocompatible therapeutic albumin/genipin bioglue designed for postoperative wound adhesion and tumour ablation [21]. Their proposed interaction with genipin is consistent with Butler's Reaction Scheme 2 (Fig. 1, [14]), which further leads to cross-linking with two genipin molecules between two BSA chains as shown in Fig. 3A [21]. This is in agreement with the cross-linking mechanism proposed by Chen et al. [16] for NOCC and genipin (Fig. 2). Additionally, Wang et al. proposed a reaction (Fig. 3B) that adheres to Butler et al.'s Reaction Scheme 1 (Fig. 1, [14]).

While both Chen et al. [16] and Wang et al. [21] drew attention to two genipin molecules i.e. genipin dimer for linking NH_2 groups, Dimida et al. who studied genipin cross-linking of chitosan [23] pointed out that under mild acidic or neutral conditions, the cross-linking reaction involves two different steps. The first is the nucleophilic attack of the amino groups of chitosan on the olefinic carbon atom at C3 of genipin. Followed by the opening of the dihydropyran ring and an attack on the carbonyl group by the newly formed secondary amine group. The second step is a nucleophilic attack of the chitosan amino group on the carboxyl genipin group with amide formation. According to Scheme B (Fig. 4), the oxygen radical-induced polymerisation of genipin could occur between genipin molecules already linked to amino groups of chitosan. This could lead to the cross-linking of chitosan chains by genipin molecules or even by genipin copolymers having a high conjugation of C═C bond, which they deem responsible for the dark-blue colour of the formed hydrogel. The proposed Scheme B in Fig. 4 resembles Scheme A in Fig. 3 [21] and the scheme in Fig. 2 [16]. Other authors also suggest the possibility of the formation of oligomers containing up to 88 genipin molecules between chitosan chains [24].

Schakowski et al. focused on BSA-coated haemoglobin and proposed NH_2 genipin interaction based on Butler et al. [14] (see Fig. 5 below) [25]. They suggested that the combination of Reaction Schemes 1 and 2 proposed by Butler et al. (Fig. 1), can lead to a single genipin molecule cross-linking with two NH_2 groups similar to Scheme A (Fig. 4) proposed by Dimida et al. [23] and contrary to the cross-linking path proposed by Wang et al. [21] (Fig. 3).

Here, we sought to improve the understanding of the genipin-BSA interaction by using fluorescence spectroscopy to generate experimental data for kinetic fitting and clarify which processes are dominant and rate relevant. Fluorescence spectroscopy has been previously shown to be valuable in studies of interactions between different molecules and serum albumin that focused on their binding ability and binding sites. [26–28] We focus on low BSA concentrations that are typically not reported because they do not form rigid hydrogel structures. Furthermore, the experimental study employs fluorescence intensity (FI) to follow the progress of the reaction [29], while the aim of modelling is to capture the kinetic profiles of the reaction, in particular, the dynamics of the onset of the reaction which under BSA concentrations studied can verify or dispute proposed reaction networks. The binding of genipin to free amino groups present on polymers such as polysaccharides (e.g. chitosan) and proteins (e.g. BSA) produce structures with conjugated double bonds, which are fluorescent in the red region (excitation peak at ~590, emission peak at ~630 nm) and are visibly dark blue in colour [23], [30–35]. Therefore, the fluorescence intensity of genipin-cross-linked polymers has been widely used to monitor the cross-linking reaction in the literature.

3. Materials and methods

3.1. Materials

Bovine serum albumin (BSA) (≥98 %, product code A7030), genipin (≥98 %, product code G4796), glacial acetic acid, sodium dodecyl sulphate (SDS) (≥98.5 %, product number L4509), 2,4,6-

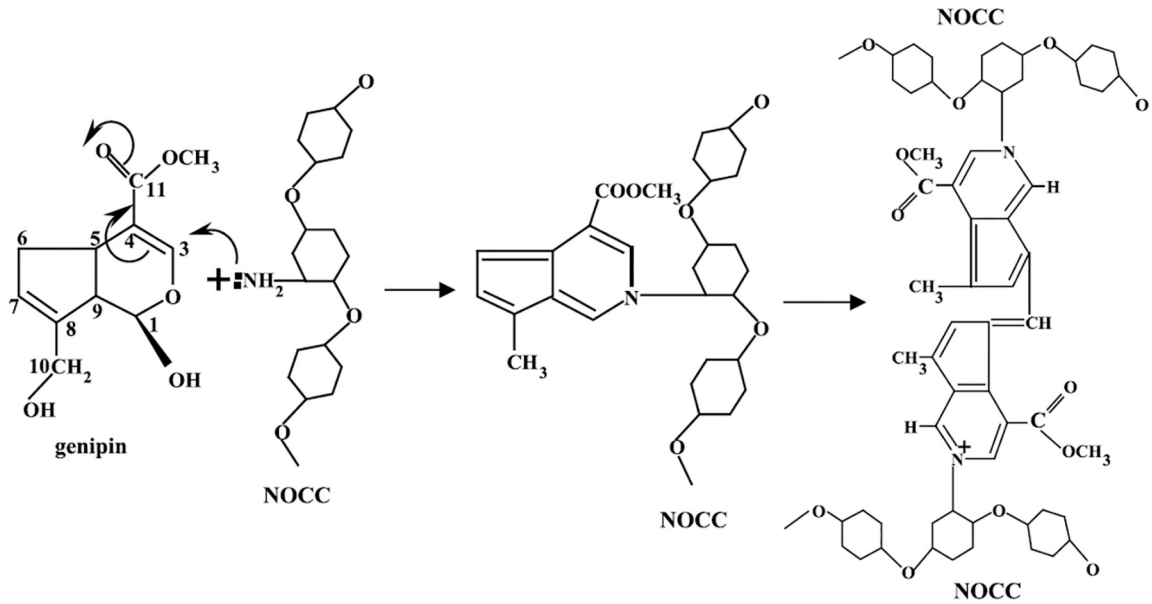

Fig. 2. Proposed reaction mechanism of genipin and NOCC. Adapted from Chen et al. [16] with permission from Elsevier.

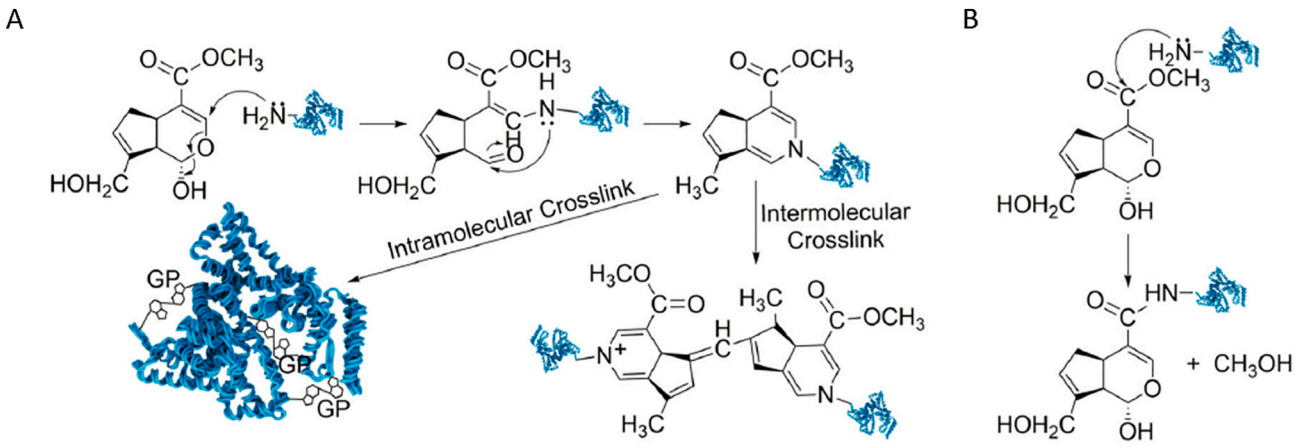

Fig. 3. Schematic representation of the reaction mechanism of genipin with BSA. Reaction A refers to the nucleophilic attack on genipin by primary amine groups forming intra- or intermolecular cross-linking structures. Reaction B refers to the nucleophilic substitution of the ester groups in genipin. Adapted from Wang et al. [21] with permission from Elsevier.

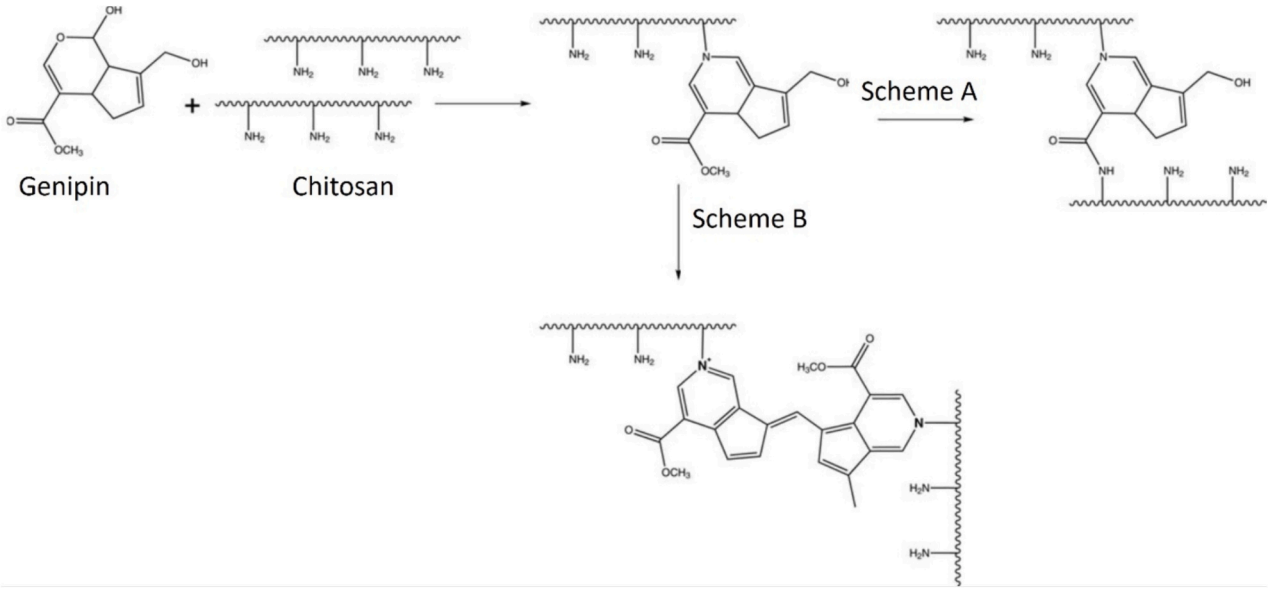

Fig. 4. Scheme of the cross-linking reactions between chitosan and genipin. Adapted from [23] with permission from John Wiley and Sons.

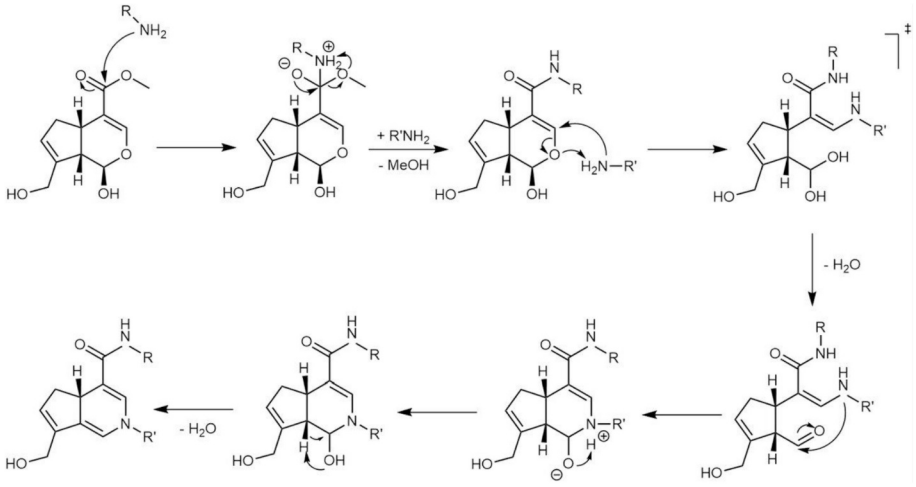

Fig. 5. Cross-linking reaction mechanism of genipin with BSA. Adapted from [25] with permission from Taylor & Francis.

trinitrobenzenesulfic acid (TNBS) (5 %, product number P2297,), glycine (≥99 %, product number G7126) were purchased from Sigma Aldrich. Hydrochloric acid 1.0 M standardised solution (CAS: 7647-01-0) and sodium hydrogen carbonate (≥99 %, CAS: 144–55-6) were purchased from Thermo Scientific Chemicals. All chemicals were used as received.

3.2. Experimental study of BSA-genipin interaction using fluorescence spectroscopy

Samples containing BSA (0.2, 1, 5, 10, 30 and 50 mg/mL) and a constant genipin concentration (0.5 mg/mL) were prepared and the FI was measured every hour over 24 h. The BSA concentration range selected for the study was a result of a preliminary FI screening aimed at establishing wide concentration range within which FI dynamics shows dependence on BSA concentration. A UV–Vis spectrophotometer (BMG LABTECH, FLUOstar Omega Microplate Reader with BMG LABTECH's Omega software) was used to measure the fluorescence of the BSA-genipin mixture. The excitation and emission wavelengths were 550 nm and 650 nm, respectively. [30,31] First, BSA and genipin solutions were prepared separately by dissolving BSA and genipin powder in deionised water to give 10 % *w/v* BSA and 1 % *w/v* genipin stock solutions. The BSA-genipin samples to be analysed were prepared by stirring the BSA and genipin solutions together for ~5 min. The sample mixture was transferred to microplate wells (0.5 mL per well) for FI measurements at 37 °C. A Vision Plate™ 24 microplate was used to contain the samples and transparent plastic covers were used to seal the microplates to prevent moisture evaporation from the samples which would lead to a change in concentration during the measurement. The measurement was carried out for 24 h using the well scan mode (one well scanned per sample per hour). For each well scan, a matrix of 10 × 10 data points was scanned with 20 flashes per scan point which were then averaged to give a single value for each scan point. There was a 0.1 s settling time between scan points which is the time before the measurement begins after the well has come to the measurement position. A bottom-up measurement was used, where both the excitation source and the detector were located beneath the microplate. A bottom-up measurement (rather than a top-down one) was chosen to avoid potential issues with condensation on the covering foil which affects the measurement from the top of the sample. The FI of deionised water, BSA and genipin solutions were also measured over 24 h to establish a baseline and were confirmed to remain approximately constant and negligible (<500 AU). They were therefore considered inconsequential to the interpretation of FI data in this study.

3.3. Experimental study of BSA-genipin interaction in the presence of acid using fluorescence spectroscopy

The same experiment described in Section 3.2 was conducted in the presence of acetic acid (at constant concentration of 1.75×10^{-2} mol/dm^3). Genipin stock solution was prepared by dissolving 1 % *w/v* genipin in 1 % *v/v* acetic acid in deionised water and samples with a constant genipin concentration of 0.5 mg/mL were prepared as detailed in Section 3.2. BSA concentrations and fluorescence measurements were described in Section 3.2.

3.4. Estimation of the initial concentration of reactive amine groups in BSA

While the total number of amino acid building blocks in BSA is known and their concentration can be calculated theoretically from the molecular weight of BSA (see Section 1 in the Supplementary Material), the question to answer is how many of these amino acid residues contain reactive NH_2 groups, i.e. amino groups available for the reaction with genipin. The concentration of reactive NH_2 groups in BSA was estimated using 2,4,6-trinitrobenzenesulfonic acid (TNBS) as the key reagent in a well-established method for the quantification of primary amine groups on small molecules such as amino acids as well as on larger molecule proteins [36]. Briefly, BSA samples were prepared by dissolving BSA powder in a 0.1 M sodium bicarbonate solution. Then, the BSA solutions were mixed with 0.01 % *w/v* TNBS and incubated for 2 h at 40 °C, after which 10 % *w/v* SDS and 1 M HCl were added to the mixture in a volume ratio of BSA:TNBS:SDS:HCl = 4:2:2:1. The primary amine once reacted with TNBS yields a highly chromogenic derivative. Its concentration can be determined using the Beer-Lambert law by measuring its absorbance at 335 nm using a UV–Vis spectrophotometer (BMG LABTECH, FLUOstar Omega Microplate Reader with BMG LABTECH's Omega software). To produce a calibration curve the amino acid, glycine, dissolved in the sodium bicarbonate solution at pre-determined concentrations (1, 2, 4, 6, 8, and 10 μg/mL) was reacted with TNBS (Fig. S2 and S3, Supplementary Material) and their absorbances at 335 nm were measured with the UV–vis spectrophotometer. Absorbance against concentration was plotted and the resulting calibration curve (Fig. S4, Supplementary Material) was subsequently used to determine the concentration of reactive NH_2 groups in BSA. This, in turn, was used as the initial amino group concentration in the modelling study. Glycine was selected because it is the smallest amino acid (containing one primary amino group) with a known structure and molecular weight. Detailed procedures are provided in the Supplementary Material.

3.5. Mathematical modelling study and kinetic fitting

To elucidate the potential mechanisms underlying the process of genipin cross-linking with BSA, several reaction networks were explored. Reaction networks based on the literature (Section 2) were initially modelled, modified and expanded to better match the experimentally captured trends. Each reaction network was mathematically described using a system of ordinary differential equations (ODEs) derived based on mass action kinetics, which is commonly used in chemical kinetics studies. The validity of these reaction networks was subsequently assessed through a comprehensive evaluation of their ability to accurately match the full set of experimental data (without and with acid addition) i.e. using a single set of estimated rate constants. To achieve this, an appropriate fitting procedure was developed, allowing for the comparison between the experimental data using different initial concentrations of BSA and the concentrations obtained by solving the ODEs that represent the considered reaction networks. To facilitate the comparison between the experimental data which measured FI, and the ODE results which gave the concentrations of the chemical species involved, the raw experimental data needed to be transformed into concentrations. Given that there is no direct functional relationship between FI and concentration units specific assumptions were made and a series of steps were taken to perform the required conversions.

In the numerical simulations, the FI was represented as a linear combination of the concentrations of selected chemical species (Eq. 1). This approach allowed meaningful comparisons and facilitated the assessment of the proposed reaction networks against the experimental data.

$$I_{num} = \sum \alpha_i c_i \tag{1}$$

where c_i is the concentration of the i-th species while α_i represents its contribution. Next, both the fluorescence signal obtained in the numerical simulations and that obtained in the experiment were normalised using the *Z*-normalisation method through the formula shown in Eq. 2–3.

$$y_{num,i} = \frac{I_{num,i} - \mu_{num,i}}{\sigma_{num,i}} \tag{2}$$

$$y_{exp,i} = \frac{I_{exp,i} - \mu_{exp,i}}{\sigma_{exp,i}} \tag{3}$$

where μ_i and σ_i are defined as:

$$\mu_i = \frac{1}{N}\sum_{i=1}^{N} I_i \tag{4}$$

$$\sigma_i = \sqrt{\frac{1}{N-1}\sum_{i=1}^{N}(I_i - \mu_i)^2} \tag{5}$$

In the previous equations, the subscripts "exp" and "num" refer to data obtained from experiments and numerical simulations, respectively. The primary objective was to assess whether the proposed model could generate curves that correspond exactly to those acquired experimentally. To achieve this goal, the parameters that best fit the experimental and numerical data were determined by solving a nonlinear least squares problem. This optimisation process was carried out using a MATLAB code specifically developed for this purpose. The system of ordinary differential equations (ODEs) corresponding to the models under consideration was solved using the ode15s function, a numerical solver commonly employed for stiff ODEs. Subsequently, the nonlinear least squares problem was solved using the fminsearch function which efficiently finds the optimal parameter values that minimise the discrepancy between the experimental and numerical datasets.

4. Results and discussion

BSA and genipin mixtures with varying concentrations of BSA (0.2–50 mg/mL) and a fixed concentration of genipin (0.5 mg/mL) were studied by recording the change in FI over time (Section 3.2, Fig. 6). Fluorescence imaging offers superior sensitivity which is particularly important when the process is studied at low concentrations. [37] The technique is non-invasive allowing in-situ monitoring of the genipin-NH_2 groups interaction over an extended time period. While the genipin solution is colourless, the BSA solution is pale yellow. When they are mixed and the reaction begins to proceed, the colour of the mixture which corelates with the increase in FI gradually turns dark blue. This colour (and FI) change has been reported to correlate with the formation of a hydrogel-like structure when very high concentrations of BSA are used (approximately 100 mg/mL BSA and 5 mg/mL genipin), indicating the occurrence of the cross-linking reaction [19,21]. For the concentration range shown in Fig. 6, the change in FI was recorded and a colour change was observed, however hydrogels did not form. From Fig. 6, it can be noted that an increase in the initial concentration of BSA yields an increase in FI, while the individual fluorescence intensities over time follow a similar trend as expected from a concentration vs. time graph. Initially following a slow start, there is a steep increase in FI (for concentrations 5–50 mg/mL) followed by a plateau, which is concentration-dependent. At lower concentrations of BSA (below 30 mg/mL) the plateau starts at ~8–10 h, indicating the end of the BSA-genipin reaction. In the case of the 5 and 10 mg/mL runs the plateau has a downward trend which may indicate a quenching effect or given the low concentrations of BSA, breakdown of the links in product/s responsible for observed fluorescence. At higher BSA concentrations (30 and 50 mg/mL) the plateau is not observed and only a slowing of the FI increase can be seen which suggests the reaction was incomplete for the duration it was monitored.

In the presence of acetic acid a similar trend of FI was recorded (Fig. 7). Higher concentrations (30 A and 50 A mg/mL, where A following the concentration of BSA indicates the presence of acid) reach similar values for FI as seen in Fig. 6, but more rapidly. A plateau occurs at ~10–12 h, followed by a drop in FI after 16 h. The drop in FI at a later stage of the reaction can be postulated to be due to high fluorescence and dark colour which lead to self-quenching. However, some drop in fluorescence was also observed at a later stage of the 10 A mg/mL run. Therefore the decomposition of the product/s and reversibility of the reaction/s that yield fluorescence needs to be considered.

A direct comparison between the runs with and without the added acid, at the otherwise same experimental conditions, is given in Fig. 8. At higher BSA concentrations (30 A and 50 A mg/mL) the reaction is accelerated in the presence of acid but gives similar final values of FI at 24 h as in the case of runs without the acid addition. At BSA concentrations below 30 mg/mL the acidified samples showed less or no plateau, while the reaction started slower and accelerated at later times giving similar or higher final values of FI.

For the kinetic fitting study using the results presented in Figs. 6–8, the initial concentrations of NH_2 groups available for the reaction as well as genipin and acetic acid, first needed to be determined. Using the calibration curve generated with glycine (Fig. S4, Supplementary Material), reactive amino groups associated with BSA were measured to be 0.79 ± 0.05 % *w/w* of the total BSA weight. Using this information the initial concentrations of reactive amino groups associated with the BSA samples used in the fluorescence study are calculated and shown in Table 1. Detailed experimental and calculation procedures are given in Supplementary Material.

These results show that only approximately 5.6 % of the total number of amino acid residues associated with a BSA molecule have amino groups which are available for the reaction (Table S3, Supplementary Material). This figure is in agreement with the literature which shows that BSA possesses 30–35 lysine ε-amino groups (out of a total of 59) that are typically available for derivatisation. [38,39] If 30–35 of the 583 amino acid residues are free to react this gives a value of 5–6 % which is in good agreement with the 5.6 % value obtained from the experimental assay. The initial concentration of genipin was kept constant at 0.5 mg/mL, equating to 2.21×10^{-3} mol/dm^3. When acetic acid was added, the

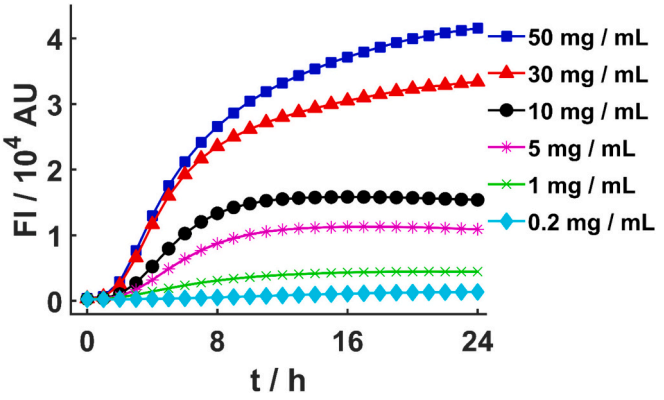

Fig. 6. Fluorescence intensity change over time with varying BSA concentrations (0.2–50 mg/mL) in the presence of constant genipin concentration (0.5 mg/mL).

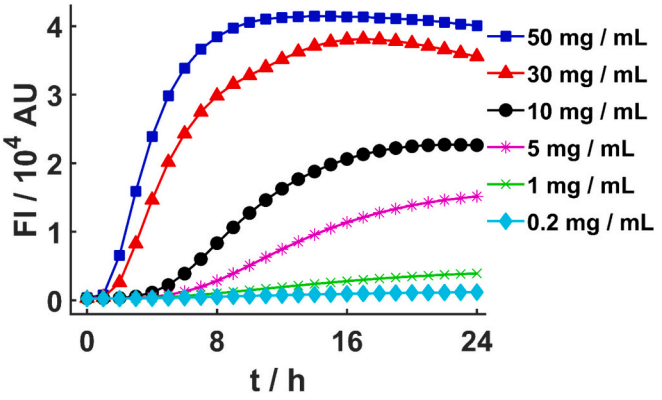

Fig. 7. Fluorescence intensity change over time with varying BSA concentrations (0.2–50 mg/mL), in the presence of constant genipin concentration (0.5 mg/mL) and a constant concentration of acetic acid (1.75×10^{-2} mol/dm^3).

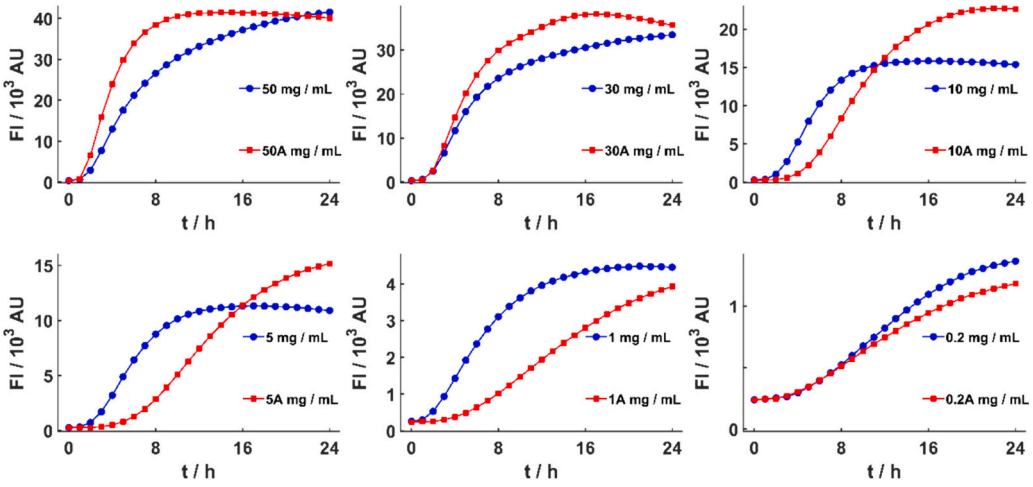

Fig. 8. Fluorescence intensity change over time with varying BSA concentrations (0.2–50 mg/mL), in the presence of constant genipin concentration (0.5 mg/mL), with or without 1.75×10^{-2} mol/dm^3 acetic acid (acidified samples are denoted with A).

Table 1
Initial concentrations of NH_2 groups available for reaction (reactive NH_2 groups), calculated using calibration curve produced using glycine.

[BSA] (mg/mL)	$[NH_2]_{reactive}$ (mg/mL)	$[NH_2]_{reactive}$ (mol/dm^3)
0.2	1.58×10^{-3}	9.87×10^{-5}
1	7.9×10^{-3}	4.94×10^{-4}
5	3.95×10^{-2}	2.47×10^{-3}
10	7.90×10^{-2}	4.94×10^{-3}
30	2.37×10^{-1}	1.48×10^{-2}
50	3.95×10^{-1}	2.47×10^{-2}

initial acid concentration was kept constant at 1.75×10^{-2} mol/dm^3.

To identify the reaction mechanism that gives good agreement with the experimental data, several reaction networks were considered. The initial reactions considered are based on the literature (Section 2) and are given in Table 2. Based on the previously proposed theory different subsets of these reactions are modelled.

The commonly assumed reaction mechanism for the reaction of genipin and amino groups interaction has only two summative steps. The first being nucleophilic attack at C3 by the amine group, which is represented by R1.1 in Table 2, which leads to the formation of the intermediate Int_1. Followed by Int_1 proceeding to form $(Gen)_2(NH_2)_2$ through the second reaction, R1.2. To test the applicability of this model two scenarios were investigated. In the first case, the fluorescence is considered to result from the formed $(Gen)_2(NH_2)_2$, while in the second case, it is considered to result from both Int_1 and $(Gen)_2(NH_2)_2$. The analysis shows that while neither of the two scenarios of this model produces a close fit, the first case gives better results and is shown in Fig. 9. At $t = 0$ the standardised experimental and estimated values differ due to the procedure used to normalise the experimental and numerical data. Furthermore, while the model describes the experimental results to a certain degree it cannot provide a satisfactory agreement for all the experiments simultaneously using the same set of parameters. The best fit was obtained for BSA concentrations of 30 and 50 mg/mL while the model could not give satisfactory results for the concentration range of 1.0–10 mg/mL. The rate constants (Fig. 9) indicate that the formation of the intermediate Int_1, i.e. the first linkage of the genipin and NH_2 groups, is a faster process compared to the second step which showcases a cross-linking reaction. This agrees with Butler et al. who found that a nucleophilic attack on genipin by a primary amine group, leading to the formation of a heterocyclic compound, is a faster step [14].

Table 2
Literature-based reactions proposed to take place between genipin and NH_2 groups available on BSA.

$NH_2 + Gen \xrightarrow{k_{1.1}} Int_1$	$r_{1.1} = k_{1.1}[NH_2][Gen]$	(R1.1)
$2Int_1 \xrightarrow{k_{1.2}} (Gen)_2(NH_2)_2$	$r_{1.2} = k_{1.2}[Int_1]^2$	(R1.2)
$NH_2 + Int_1 \xrightarrow{k_{1.3}} Gen(NH_2)_2$	$r_{1.3} = k_{1.3}[NH_2][Int_1]$	(R1.3)
$NH_2 + Gen \xrightarrow{k_{1.4}} Int_2$	$r_{1.4} = k_{1.4}[NH_2][Gen]$	(R1.4)
$NH_2 + Int_2 \xrightarrow{k_{1.5}} Gen(NH_2)_2{}^*$	$r_{1.5} = k_{1.5}[NH_2][Int_2]$	(R1.5)

A further modelling study considered a reaction network consisting of R1.1 and R1.3 (Table 2) and a reaction network consisting of R1.4 and R1.5, with the later representing the nucleophilic substitution of the ester group in genipin and the formation of Int_2, followed by the cross-linking process via further reaction of Int_2 with a single NH_2 group (R1.5). Similarly, R1.3 represents a cross-linking process via further reaction of Int_1 with a single NH_2 group. From a chemical kinetics perspective, the individual reaction network consisting of R1.1 and R1.3 does not differ from the network consisting of R1.4 and R1.5, although they represent two different processes. The same set of parameters gives the best fit in both cases (Fig. 10). In the case of the reaction mechanism consisting of R1.1 and R1.3 the fluorescence was assumed to be the result of Int_1 and $Gen(NH_2)_2$. In the case of the mechanism consisting of R1.4 and R1.5 the fluorescence was assumed to be the result of Int_2 and $Gen(NH_2)_2$*, where * denotes the difference in the structure of this product compared to that formed in R1.3. Similar to the trends seen in Fig. 9, the best fit was achieved for BSA concentrations of 30 and 50 mg/mL with the discrepancies at the initial stages of the reaction remaining.

Since all the previously studied reaction networks showed the potential to fit some experimental data, a model combining all these reactions into one network (R1.1-R1.5, Table 2) was explored next. In this case, the fluorescence was assumed to be a result of Int_1, Int_2, $(Gen)_2(NH_2)$, $Gen(NH_2)_2$ and $Gen(NH_2)_2$*. As shown in Fig. 11 it was found that this model produces improved agreement with the experimental results. However, satisfactory fit of the trends experimentally captured in the initial 2 h of the reaction was not achieved and neither was the model able to account for the decrease in FI captured experimentally in the runs employing BSA concentrations of 5 and 10 mg/mL.

This model was further tested with the experimental data obtained when acetic acid was present in the system (Fig. 7). The fit was encouraging (Fig. 12), however, the drop in FI experimentally captured in the runs employing BSA concentrations of ≥30 mg/mL was not replicated. Comparing the results with and without the acid the values of the rate constants and α_i coefficients differ in two cases. This could be attributed to a different concentration distribution between the species contributing to the fluorescence signal due to the presence of acid in one

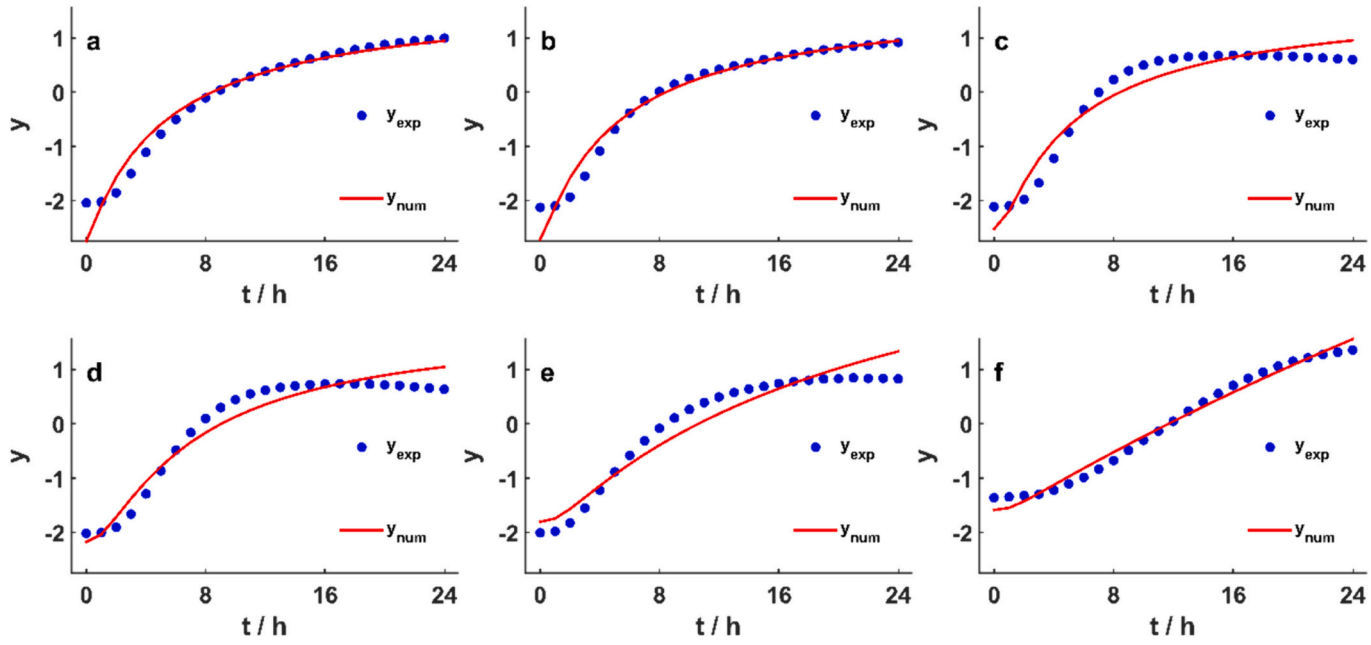

Fig. 9. Results of the fitting for the sub-model consisting of the reaction R1.1 and R1.2 with the following concentrations of BSA: a) 50 mg/mL, b) 30 mg/mL, c) 10 mg/mL, d) 5 mg/mL, e) 1 mg/mL, and f) 0.2 mg/mL. Parameters used in simulations: $k_{1.1} = 6.28 \times 10^2$ mol^{-1} L h^{-1}; $k_{1.2} = 4.20 \times 10^1$ mol^{-1} L h^{-1}; $\alpha_1 = 1.0$.

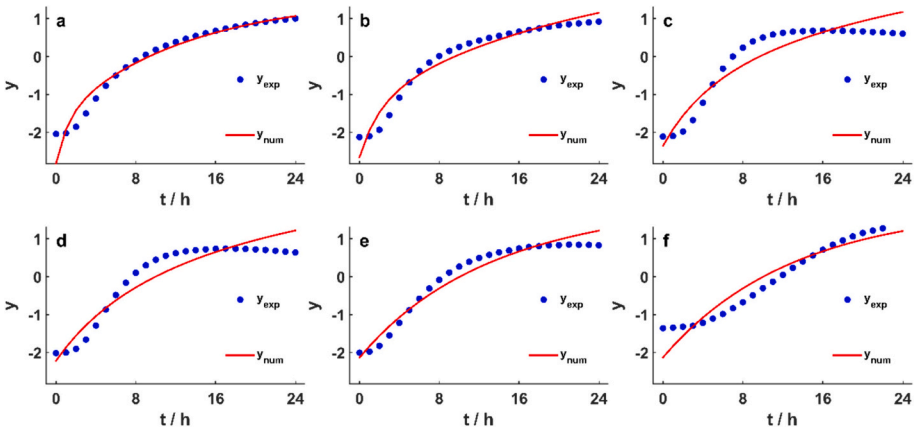

Fig. 10. Results of the fitting for sub-models consisting of the reactions (R1.1, R1.3) and (R1.4, R1.5): a) 50 mg/mL, b) 30 mg/mL, c) 10 mg/mL, d) 5 mg/mL, e) 1 mg/mL, and f) 0.2 mg/mL. Parameters used in simulations: $k_{1.1} = 3.50 \times 10^1$ mol^{-1} L h^{-1}; $k_{1.3} = 3.45$ mol^{-1} L h^{-1}; $k_{1.4} = 3.50 \times 10^1$ mol^{-1} L h^{-1}; $k_{1.5} = 3.45$ mol^{-1} L h^{-1}; $\alpha_1 = 1.20 \times 10^3$; $\alpha_2 = 3.70 \times 10^3$.

case.

To simultaneously address notable differences in the initial stages of the process, in particular in the absence of acetic acid where the model did not reproduce the experimentally captured S-shaped curve and the decrease in FI observed in some experiments, a new model involving feedback cycles of NH_2 and Gen has been constructed. A feedback loop was considered due to its common association with a S-shaped curve. [40] The model is based on the observed slow rate of cross-linking processes using genipin [29] and the postulation of an initial reaction R2.1 (Table 3) required to activate genipin prior to further reacting with NH_2 groups. Subsequently, similar to what has been proposed in previously studied models, activated genipin proceeds to react with NH_2 groups to form Int_3 (R2.2), which then proceeds to react with available reactive NH_2 groups to form $Gen(NH_2)_2$** (R2.3). Where ** denotes a potentially structurally different product compared to the products discussed above. Importantly, to secure the feedback loop it is proposed that Int_3 can revert back (e.g. decompose) to unreactive genipin and amine (R2.4). It should be noted that the proposed reaction network focuses on summative processes rather than detailed reaction mechanisms in an attempt to kinetically match experimentally captured trends in fluorescence intensity. In the case of this model fluorescence was assumed to be the result of both Int_3 and $Gen(NH_2)_2$**.

The simulation study employing the feedback cycle of NH_2 and Gen showed all the important features of the experimental curves (Fig. 13). This model improved the fit in the regions of the experimental curves that the previous models could not. This is most evident at lower BSA concentrations (Fig. 13e and f). Although the fitted curves show some deviations in the initial stages of the experiments for BSA concentrations of 5–50 mg/mL (Fig. 13a-d), in general for all the runs data recorded beyond 2 h are fitted quite well.

Further confirmation of the model's validity was obtained by fitting the experimental data recorded in the presence of acetic acid. The results are shown in Fig. 14. Similar to the fitting results presented in Fig. 12, the presence of the acid improves the proposed model's ability to fit the experimental curves. The model could now fit all regions of the curves obtained in the experiments, including the FI drop recorded in 30 A and

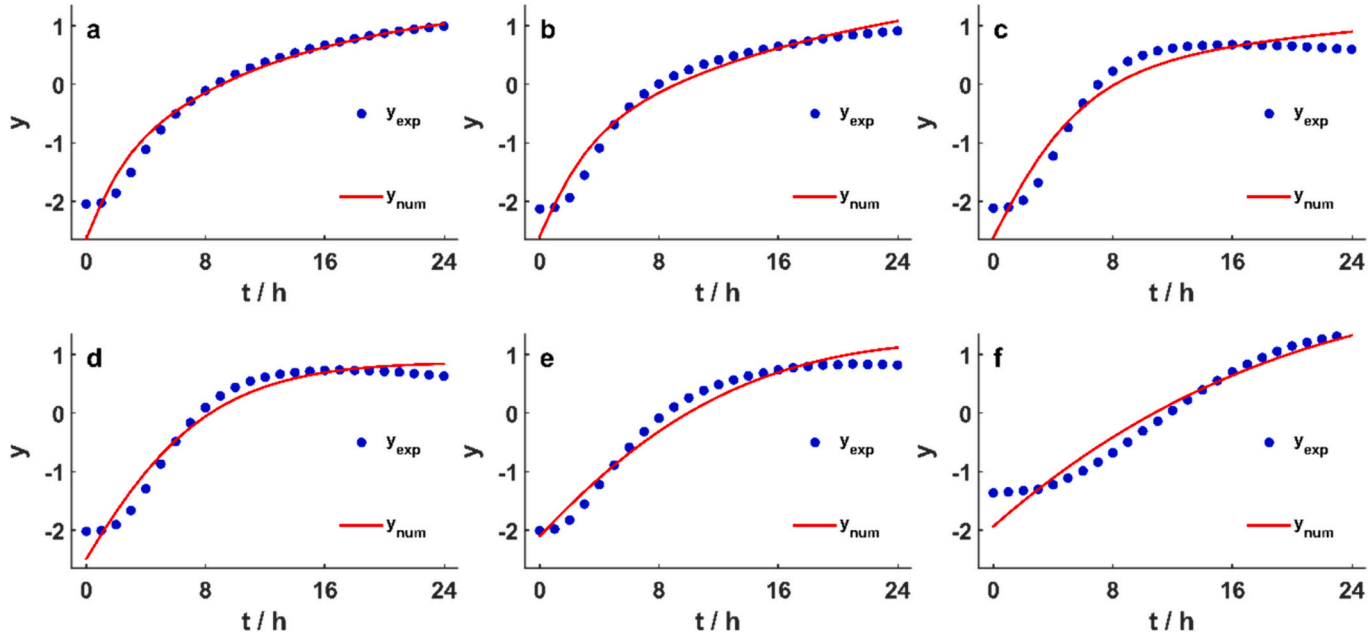

Fig. 11. Results of the fitting for the model presented in Table 2, at BSA concentration of: a) 50 mg/L, b) 30 mg/mL, c) 10 mg/mL, d) 5 mg/mL, e) 1 mg/mL, and f) 0.2 mg/mL. Parameters used in simulations: $k_{1.1} = 8.66\ mol^{-1}\ L\ h^{-1}$; $k_{1.2} = 1.04 \times 10^{4}\ mol^{-1}\ L\ h^{-1}$; $k_{1.3} = 9.53 \times 10^{6}\ mol^{-1}\ L\ h^{-1}$; $k_{1.4} = 1.09 \times 10^{-1}\ mol^{-1}\ L\ h^{-1}$; $k_{1.5} = 3.08\ mol^{-1}\ L\ h^{-1}$; $\alpha_1 = 6.54 \times 10^{7}$; $\alpha_2 = 4.42 \times 10^{6}$; $\alpha_3 = 1.96 \times 10^{6}$; $\alpha_4 = 2.54 \times 10^{8}$; $\alpha_5 = 1.07 \times 10^{2}$.

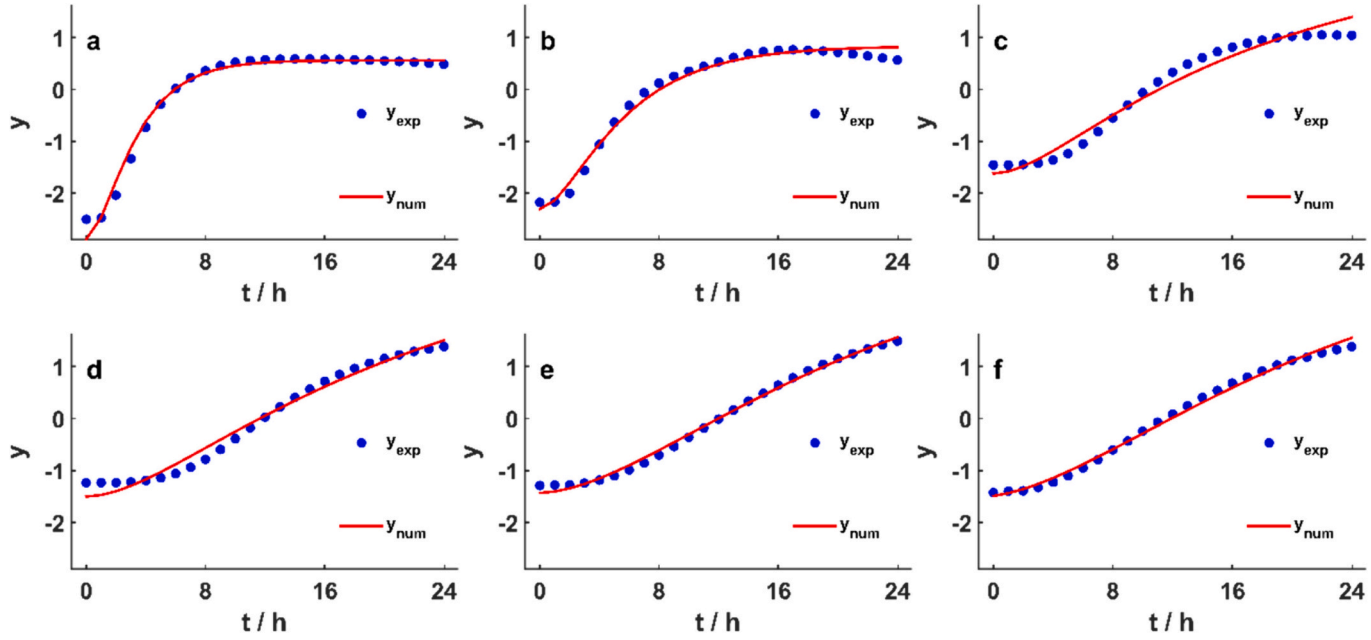

Fig. 12. Results of the fitting of the model presented in Table 2 in the presence of acetic acid, at BSA concentrations of: a) 50 mg/mL, b) 30 mg/mL, c) 10 mg/mL, d) 5 mg/mL, e) 1 mg/mL, and f) 0.2 mg/mL. Parameters used in simulations: $k_{1.1} = 7.85 \times 10^{-3}\ mol^{-1}\ L\ h^{-1}$; $k_{1.2} = 9.45 \times 10^{4}\ mol^{-1}\ L\ h^{-1}$; $k_{1.3} = 2.12 \times 10^{1}\ mol^{-1}\ L\ h^{-1}$; $k_{1.4} = 2.70 \times 10^{-01}\ mol^{-1}\ L\ h^{-1}$; $k_{1.5} = 2.30\ mol^{-1}\ L\ h^{-1}$; $\alpha_1 = 1.54 \times 10^{9}$; $\alpha_2 = 3.66 \times 10^{2}$; $\alpha_3 = 8.41 \times 10^{5}$; $\alpha_4 = 5.73 \times 10^{11}$; $\alpha_5 = 5.73 \times 10^{1}$.

Table 3
Mechanism employing feedback loop.

$Gen \xrightarrow{k_{2.1}} Gen^{*}$	$r_{2.1} = k_{2.1}[Gen]$	(R2.1)
$NH_2 + Gen^{*} \xrightarrow{k_{2.2}} Int_3$	$r_{2.2} = k_{2.2}[NH_2][Gen^{*}]$	(R2.2)
$NH_2 + Int_3 \xrightarrow{k_{2.3}} Gen(NH_2)_2{}^{**}$	$r_{2.3} = k_{2.3}[NH_2][Int_3]$	(R2.3)
$Int_3 \xrightarrow{k_{2.4}} NH_2 + Gen$	$r_{2.4} = k_{2.4}[Int_3]$	(R2.4)

50 A mg/mL runs. Being able to model acidified conditions is important when chitosan is used, as chitosan is readily prepared in acidified solutions to aid its solubility leading to acidified conditions during hydrogel synthesis. The model is also supported by Chen et al. [16] who studied BSA encapsulation and release from *N,O*-carboxymethyl chitosan (NOCC), alginate and genipin cross-linked pH-responsive hydrogels and showed that the release is possible and dependant on the environmental pH, suggesting that linking of BSA-genipin can be reversed so that BSA can be released. As with the previous model, which compared results with and without the acid, the parameter values differ likely due

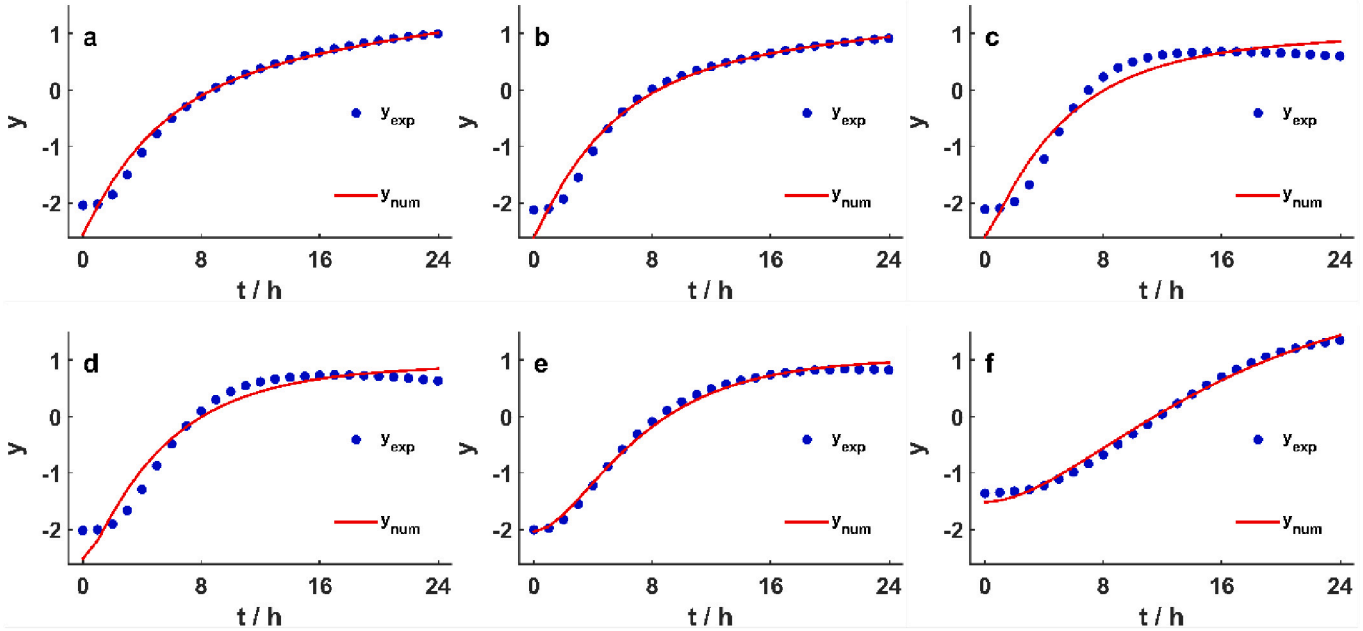

Fig. 13. Results of the fitting of the model presented in Table 3, at BSA concentrations of: a) 50 mg/mL, b) 30 mg/mL, c) 10 mg/mL, d) 5 mg/mL, e) 1 mg/mL, and f) 0.2 mg/mL. Parameters used in simulations: $k_{2.1} = 9.51 \times 10^{-7}$ h^{-1}; $k_{2.2} = 8.04 \times 10^{2}$ mol^{-1} L h^{-1}; $k_{2.3} = 4.74 \times 10^{-1}$ mol^{-1} L h^{-1}; $k_{2.4} = 1.83 \times 10^{-1}$ h^{-1}; $\alpha_1 = 1.00$; $\alpha_2 = 1.00$.

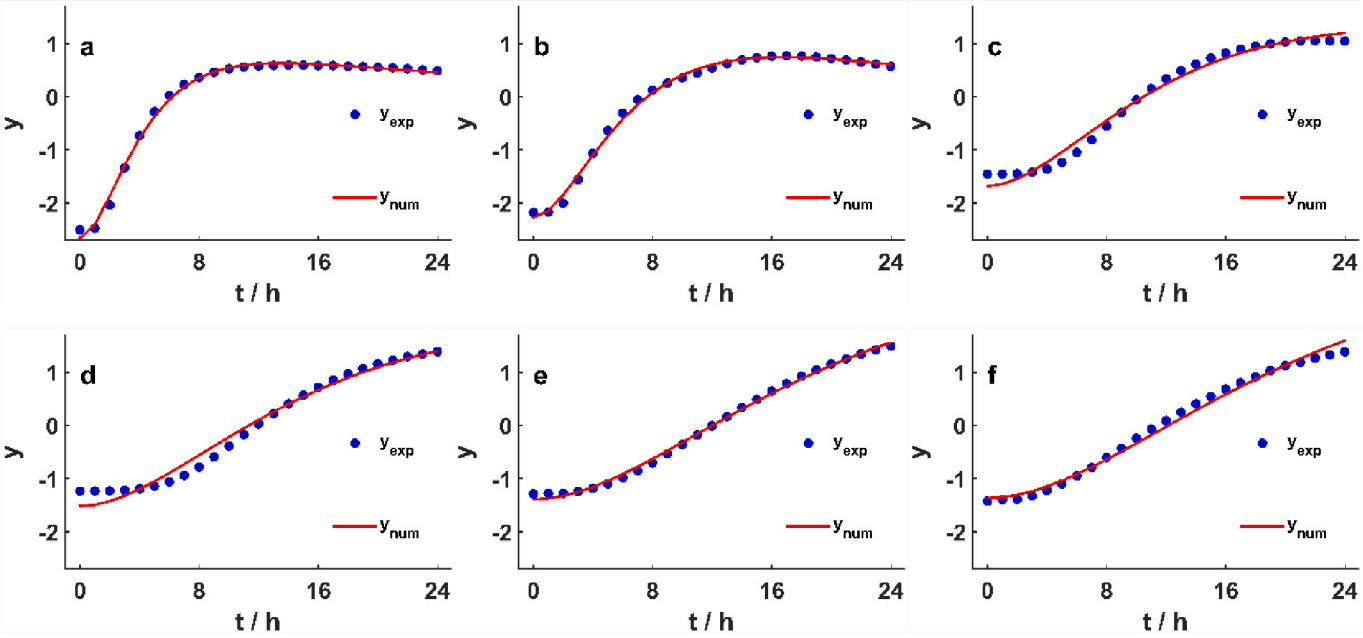

Fig. 14. Results of the fitting procedure of the reaction network presented in Table 3 in the presence of acid, at BSA concentrations of: a) 50 mg/mL, b) 30 mg/mL, c) 10 mg/mL, d) 5 mg/mL, e) 1 mg/mL, and f) 0.2 mg/mL. Parameters used in simulations: $k_{2.1} = 7.70 \times 10^{-2}$ h^{-1}; $k_{2.2} = 2.04 \times 10^{1}$ mol^{-1} L h^{-1}; $k_{2.3} = 1.27 \times 10^{1}$ mol^{-1} L h^{-1}; $k_{2.4} = 4.50 \times 10^{-2}$ h^{-1}; $\alpha_1 = 1.39 \times 10^{4}$; $\alpha_2 = 2.05 \times 10^{3}$.

to a different concentration distribution of chemical species that produce fluorescence signals as a result of the presence of acid in the system.

5. Conclusions

The paper reports the experimental and kinetic modelling study of the reaction between 0.2 and 50 mg/mL BSA (as a model protein drug) and 0.5 mg/mL genipin (as a cross-linker commonly used for chitosan-based hydrogels). When chitosan is used, it is commonly firstly dissolved in 1 % *v/v* acetic acid solution and therefore the effect of the addition of acetic acid on the reaction between BSA and genipin was also evaluated. The study focused on the lower concentrations of BSA in order to capture the reaction dynamics at the onset of the BSA and genipin reaction. Genipin can engage amino groups in protein/peptide drugs and understanding this reaction is important for the effective formulation of such drugs into hydrogels involving genipin. Experimentally, the reaction is successfully followed by recording FI at excitation and emission wavelengths of 550 nm and 650 nm, respectively. The results showed that FI increases with increasing BSA concentration, with the distinctive S-shaped time series marked by a slow initial

increase in FI which then subsequently accelerates, typical of processes with a feedback loop (e.g., autocatalytic processes). In some cases (5 and 10 mg/mL of BSA runs without the addition of acetic acid and BSA ≥10 mg/mL in the case of acidified runs), a decrease in FI was captured in the later stages of the experiments. The kinetic models proposed to date [14,16], [19–21] could not produce a satisfactory fit of the S-shaped curve particularly in the initial stages of the reaction, nor could they follow a drop in FI captured in some runs. While a decrease in FI could result from the quenching effect, due to it being observed at the lower range of BSA concentrations decomposition of the fluorescent species was considered more likely. Once the model was adjusted to include the feedback cycle of both reactive NH_2 and Gen (Table 3), improved fit for both data sets (with and without the addition of acetic acid) was achieved, with the model performing better for acidified conditions capturing both S-shaped curves and drop in FI. The addition of acetic acid had a significant influence altering the dynamic of the BSA-genipin reaction and offering an additional parameter that could be used to manipulate competing processes in the case of protein encapsulation in hydrogels. For example, experimental data using 5 mg/mL of BSA show that the slow period of the reaction is extended by the addition of acid. In the case of chitosan-genipin hydrogel syntheses, this could be used to promote hydrogel cross-linking at the expense of protein drug-genipin interactions. As a result, this would yield physical (rather than chemical) protein encapsulation and release. Furthermore, the recorded drops in FI which the final model links with reversibility of the processes forming a fluorescent product, further indicate the feasibility of the release of protein drug, even after it was initially chemically linked with genipin.

CRediT authorship contribution statement

Djurdja Vukajlovic: Writing – review & editing, Writing – original draft, Methodology, Investigation, Conceptualization. **Rory Timmons:** Writing – review & editing, Writing – original draft, Investigation, Conceptualization. **Stevan Macesic:** Writing – review & editing, Writing – original draft, Supervision, Software, Resources, Methodology, Investigation, Conceptualization. **John Sanderson:** Writing – review & editing, Conceptualization. **Fengwei Xie:** Writing – review & editing, Conceptualization. **Tarek M. Abdelghany:** Writing – review & editing, Conceptualization. **Emma Smith:** Writing – review & editing, Conceptualization. **Wing Man Lau:** Writing – review & editing, Supervision, Resources, Conceptualization. **Keng Wooi Ng:** Writing – review & editing, Supervision, Resources, Conceptualization. **Katarina Novakovic:** Writing – review & editing, Writing – original draft, Supervision, Resources, Methodology, Investigation, Conceptualization.

Declaration of competing interest

The authors declare the following financial interests/personal relationships which may be considered as potential competing interests: Katarina Novakovic reports financial support was provided by The Northern Accelerator. Stevan Macesic reports financial support was provided by Ministry of Science, Technological Development and Innovation of the Republic of Serbia. If there are other authors, they declare that they have no known competing financial interests or personal relationships that could have appeared to influence the work reported in this paper.

Data availability

Data will be made available on request.

Acknowledgements

This work was supported by The Northern Accelerator (NACCF-271) and the Ministry of Science, Technological Development and Innovation of the Republic of Serbia (contract number 451-03-47/2023–01/200146) and Science Fund of the Republic of Serbia (grant number 7743504).

Appendix A. Supplementary data

Supplementary data to this article can be found online at https://doi.org/10.1016/j.ijbiomac.2024.133850.

References

[1] D. Jain, S.S. Mahammad, P.P. Singh, R. Kodipyaka, A review on parenteral delivery of peptides and proteins, Drug Dev. Ind. Pharm. 45 (9) (2019) 1403–1420.
[2] Q. Zhu, Z. Chen, P.K. Paul, Y. Lu, W. Wu, J. Qi, Oral delivery of proteins and peptides: challenges, status quo and future perspectives, Acta Pharm. Sin. B 11 (8) (2021) 2416–2448.
[3] S. Sohail, Oral Proteins and Peptides Market Size, Share | Industry Forecast 2028, 2018. https://www.alliedmarketresearch.com/oral-proteins-peptides-market. (Accessed 5th June 2023).
[4] E. Moroz, S. Matoori, J.C. Leroux, Oral delivery of macromolecular drugs: where we are after almost 100years of attempts, Adv. Drug Deliv. Rev. 101 (2016) 108–121.
[5] W. Li, J. Tang, D. Lee, T.R. Tice, S.P. Schwendeman, M.R. Prausnitz, Clinical translation of long-acting drug delivery formulations, Nature Reviews Materials 7 (5) (2022) 406–420.
[6] J. Li, D.J. Mooney, Designing hydrogels for controlled drug delivery, Nat. Rev. Mater. 1 (12) (2016).
[7] N.T.N. Vo, L. Huang, H. Lemos, A.L. Mellor, K. Novakovic, Genipin-crosslinked chitosan hydrogels: preliminary evaluation of the in vitro biocompatibility and biodegradation, J. Appl. Polym. Sci. 138 (34) (2021) 50848.
[8] A.C. Daly, L. Riley, T. Segura, J.A. Burdick, Hydrogel microparticles for biomedical applications, Nat. Rev. Mater. 5 (1) (2020) 20–43.
[9] Y. Yang, R. Zhou, Y. Wang, Y. Zhang, J. Yu, Z. Gu, Recent advances in oral and transdermal protein delivery systems, Angew. Chem. Int. Ed. 62 (10) (2023) e202214795.
[10] S.L. Reay, E.L. Jackson, D. Salthouse, A.M. Ferreira, C.M.U. Hilkens, K. Novakovic, Effective endotoxin removal from chitosan that preserves chemical structure and improves compatibility with immune cells, Polymers 15 (7) (2023) 1592.
[11] N.T.N. Vo, L. Huang, H. Lemos, A. Mellor, K. Novakovic, Poly(ethylene glycol)-interpenetrated genipin-crosslinked chitosan hydrogels: structure, pH responsiveness, gelation kinetics, and rheology, J. Appl. Polym. Sci. 137 (41) (2020) 49259.
[12] P. Yadav, A.B. Yadav, Preparation and characterization of BSA as a model protein loaded chitosan nanoparticles for the development of protein-/peptide-based drug delivery system, Future Journal of Pharmaceutical Sciences 7 (1) (2021) 200.
[13] Z. Liu, Q. Zhou, J. Zhu, J. Xiao, P. Wan, C. Zhou, Z. Huang, N. Qiang, W. Zhang, Z. Wu, D. Quan, Z. Wang, Using genipin-crosslinked acellular porcine corneal stroma for cosmetic corneal lens implants, Biomaterials 33 (30) (2012) 7336–7346.
[14] M.F. Butler, Y.-F. Ng, P.D.A. Pudney, Mechanism and kinetics of the crosslinking reaction between biopolymers containing primary amine groups and genipin, J. Polym. Sci. A Polym. Chem. 41 (24) (2003) 3941–3953.
[15] C.J. Nwosu, G.A. Hurst, K. Novakovic, Genipin cross-linked chitosan-polyvinylpyrrolidone hydrogels: influence of composition and postsynthesis treatment on pH responsive behaviour, Adv. Mater. Sci. Eng. 2015 (2015) 621289.
[16] S.-C. Chen, Y.-C. Wu, F.-L. Mi, Y.-H. Lin, L.-C. Yu, H.W. Sung, A novel pH-sensitive hydrogel composed of N, O-carboxymethyl chitosan and alginate cross-linked by genipin for protein drug delivery, Journal of controlled release : official journal of the Controlled Release Society 96 (2) (2004) 285–300.
[17] A.J. Morgan, P. Wynn, P.A. Sheehy, Milk Proteins: Minor Proteins, Bovine Serum Albumin, and Vitamin-Binding Proteins and Their Biological Properties, Reference Module in Food Science (2021).
[18] E. Assadpour, S.M. Jafari, 1 - an overview of biopolymer nanostructures for encapsulation of food ingredients, in: S.M. Jafari (Ed.), Biopolymer Nanostructures for Food Encapsulation Purposes, Academic Press, 2019, pp. 1–35.
[19] S. Teimouri, S. Kasapis, Morphology of genipin-crosslinked BSA networks yields a measurable effect on the controlled release of vitamin B6, Food Chem. 314 (2020) 126204.
[20] N. Shahgholian, G. Rajabzadeh, B. Malaekeh-Nikouei, Preparation and evaluation of BSA-based hydrosol nanoparticles cross-linked with genipin for oral administration of poorly water-soluble curcumin, Int. J. Biol. Macromol. 104 (2017) 788–798.
[21] Y. Wang, J. Guo, B. Li, D. Li, Z. Meng, S.-K. Sun, Biocompatible therapeutic albumin/genipin bioglue for postoperative wound adhesion and residual tumor ablation, Biomaterials 279 (2021) 121179.
[22] R. Touyama, Y. Takeda, K. Inoue, I. Kawamura, T. Yatsuzuka, T. Ikumoto, T. Shingu, H. Inouye Yokoi, Studies on the blue pigments produced from Genipin and methylamine. I. Structures of the brownish-red pigments, intermediates leading to the blue pigments, Chem. Pharm. Bull. 42 (1994) 668–673.
[23] S. Dimida, C. Demitri, V.M. De Benedictis, F. Scalera, F. Gervaso, A. Sannino, Genipin-cross-linked chitosan-based hydrogels: reaction kinetics and structure-related characteristics, J. Appl. Polym. Sci. 132 (28) (2015).

[24] F.-L. Mi, S.-S. Shyu, C.-K. Peng, Characterization of ring-opening polymerization of genipin and pH-dependent cross-linking reactions between chitosan and genipin, J. Polym. Sci. A Polym. Chem. 43 (10) (2005) 1985–2000.
[25] K.M. Schakowski, J. Linders, K.B. Ferenz, M. Kirsch, Synthesis and characterisation of aqueous haemoglobin-based microcapsules coated by genipin-cross-linked albumin, J. Microencapsul. 37 (3) (2020) 193–204.
[26] Y. Wang, L. Wang, M. Zhu, J. Xue, R. Hua, Q.X. Li, Comparative studies on biophysical interactions between gambogic acid and serum albumin via multispectroscopic approaches and molecular docking, JOL 205 (2019) 210–218.
[27] L. Wang, X. Wu, Y. Yang, X. Liu, M. Zhu, S. Fan, Z. Wang, J. Xue, R. Hua, Y. Wang, Q.X. Li, Multi-spectroscopic measurements, molecular modeling and density functional theory calculations for interactions of 2,7-dibromocarbazole and 3,6-dibromocarbazole with serum albumin, Sci. Total Environ. 686 (2019) 1039–1048.
[28] Z. Zhao, T. Shi, Y. Chu, Y. Cao, S. Cheng, R. Na, Y. Wang, Comparison of the interactions of flupyrimin and nitenpyram with serum albumins via multiple analysis methods, Chemosphere 289 (2022) 133139.
[29] S. Matcham, K. Novakovic, Fluorescence imaging in Genipin crosslinked chitosan–poly(vinyl pyrrolidone) hydrogels, Polymers 8 (11) (2016) 385.
[30] Y.J. Hwang, J. Larsen, T.B. Krasieva, J.G. Lyubovitsky, Effect of genipin crosslinking on the optical spectral properties and structures of collagen hydrogels, ACS Appl. Mater. Interfaces 3 (7) (2011) 2579–2584.
[31] H.G. Sundararaghavan, G.A. Monteiro, N.A. Lapin, Y.J. Chabal, J.R. Miksan, D. I. Shreiber, Genipin-induced changes in collagen gels: correlation of mechanical properties to fluorescence, J. Biomed. Mater. Res. A 87 (2) (2008) 308–320.
[32] S.-T. Liu, H.-Y. Tuan-Mu, J.-J. Hu, J.-S. Jan, Genipin cross-linked PEG-block-poly(l-lysine)/disulfide-based polymer complex micelles as fluorescent probes and pH−/redox-responsive drug vehicles, RSC Adv. 5 (106) (2015) 87098–87107.
[33] R.A.A. Muzzarelli, Genipin-crosslinked chitosan hydrogels as biomedical and pharmaceutical aids, Carbohydr. Polym. 77 (1) (2009) 1–9.
[34] F.-L. Mi, H.-W. Sung, S.-S. Shyu, Synthesis and characterization of a novel chitosan-based network prepared using naturally occurring crosslinker, J. Polym. Sci. A Polym. Chem. 38 (15) (2000) 2804–2814.
[35] F.-L. Mi, Synthesis and characterization of a novel chitosan-gelatin bioconjugate with fluorescence emission, Biomacromolecules 6 (2) (2005) 975–987.
[36] G.T. Hermanson, Chapter 2 - Functional Targets for Bioconjugation 127-228. Chapter 3 -, The Reactions of Bioconjugation, Academic Press, Boston, 2013, pp. 229–258.
[37] C.D. Hu, T.K. Kerppola, Simultaneous visualization of multiple protein interactions in living cells using multicolor fluorescence complementation analysis, Nat. Biotechnol. 21 (5) (2003) 539–545.
[38] G.T. Hermanson, Bioconjugate Techniques, 3 ed.2013.
[39] B.X. Huang, H.-Y. Kim, C. Dass, Probing three-dimensional structure of bovine serum albumin by chemical cross-linking and mass spectrometry, J. Am. Soc. Mass Spectrom. 15 (8) (2004) 1237–1247.
[40] S. Corezzi, F. Sciortino, C. De Michele, Exploiting limited valence patchy particles to understand autocatalytic kinetics, Nat. Commun. 9 (1) (2018) 2647.